Pergamon

Neuroscience Vol. 91, No. 2, pp. 783–798, 1999

PII: S0306-4522(98)00603-4
0306-4522/99 $20.00+0.00

ASTROCYTES, OLIGODENDROGLIA, EXTRACELLULAR SPACE VOLUME AND GEOMETRY IN RAT FETAL BRAIN GRAFTS

E. SYKOVÁ,*†‡ T. ROITBAK,† T. MAZEL,*† Z. ŠIMONOVÁ*† and A. R. HARVEY§

*Department of Neuroscience, 2nd Medical Faculty, Charles University, Prague, Czech Republic

†Institute of Experimental Medicine AS CR, Prague, Czech Republic

§Department of Anatomy and Human Biology, The University of Western Australia, Nedlands, Perth, Western Australia, Australia

Abstract—Fetal neocortex or tectum transplanted to the midbrain or cortex of newborn rats develops various degrees of gliosis, i.e. increased numbers of hypertrophied, glial fibrillary acidic protein-positive astrocytes. In addition, there were patches or bundles of myelinated fibres positive for the oligodendrocyte and central myelin marker Rip, and increased levels of extracellular matrix molecules. Three diffusion parameters—extracellular space volume fraction α (α = extracellular volume/total tissue volume), tortuosity λ ($\lambda = \sqrt{D/ADC}$, where D is the free and ADC is the apparent tetramethylammonium diffusion coefficient) and non-specific uptake k'—were determined *in vivo* from extracellular concentration–time profiles of tetramethylammonium. Grafts were subsequently processed immunohistochemically to compare diffusion measurements with graft morphology. Comparisons were made between the diffusion parameters of host cortex and corpus callosum, fetal cortical or tectal tissue transplanted to host midbrain ("C- and T-grafts") and fetal cortical tissue transplanted to host cortex ("cortex-to-cortex" or C-C-grafts). In host cortex, α ranged from 0.20 ± 0.01 (layer V) to 0.21 ± 0.01 (layers III, IV and VI) and λ from 1.59 ± 0.03 (layer VI) to 1.64 ± 0.02 (layer III) (mean ± S.E.M., $n = 15$). Much higher values were found in "young" C-grafts (81–150 days post-transplantation), where $\alpha = 0.34 \pm 0.01$ and $\lambda = 1.78 \pm 0.03$ ($n = 13$), as well as in T-grafts, where $\alpha = 0.29 \pm 0.02$ and $\lambda = 1.85 \pm 0.04$ ($n = 7$). Further analysis revealed that diffusion in grafts was anisotropic and more hindered than in host cortex. The heterogeneity of diffusion parameters correlated with the structural heterogeneity of the neuropil, with the highest values of α in gray matter and the highest values of λ in white matter bundles. Compared to "young" C-grafts, in "old" C-grafts (one year post-transplantation) both α and λ were significantly lower, and there was a clear decrease in glial fibrillary acidic protein immunoreactivity throughout the grafted tissue. In C-C-grafts, α and λ varied with the degree of graft incorporation into host tissue, but on average they were significantly lower ($\alpha = 0.24 \pm 0.01$ and $\lambda = 1.66 \pm 0.02$, $n = 8$) than in young C- and T-grafts. Well-incorporated grafts revealed less astrogliosis, and α and λ values were not significantly higher than those in normal host cortex.

The observed changes in extracellular space diffusion parameters could affect the movement and accumulation of neuroactive substances and thus impact upon neuron–glia communication, synaptic and extrasynaptic transmission in the grafts. The potential relevance of these observations to human neuropathological conditions associated with acute or chronic astrogliosis is considered. © 1999 IBRO. Published by Elsevier Science Ltd.

Key words: apparent diffusion coefficient, astrocytes, extracellular matrix, gliosis, myelin, oligodendrocytes.

The extracellular space (ECS) is the microenvironment of neurons and glia. In the CNS, dynamic changes in ECS volume, geometry and ionic composition (e.g., K^+, pH, Ca^{2+}) accompany neuronal activity, glial development and ageing (for review see Ref. 62). An alteration in ECS volume and/or geometry may affect the clearance of metabolites and toxic products and will impact upon the diffusion of neuroactive substances in the ECS, which may in turn affect synaptic and extrasynaptic transmission, neuron–glia communication and ionic homeostasis.[1,16,42,62]

Glial cells are believed to play an important role in the regulation of ECS ionic composition and volume in the CNS.[62,63] During normal postnatal development, as glial cells mature, ECS diffusion parameters gradually attain adult values.[11,31,50,68] This normal pattern can be disrupted by neonatal X-irradiation, which causes cell death, blood–brain barrier damage and astrogliosis.[65] ECS characteristics also change in gliotic tissue surrounding an acute penetrating CNS injury.[52] These observations raise the important question of how changes in glial cell phenotype during ageing and in different

‡To whom correspondence should be addressed.

Abbreviations: BBB, blood–brain barrier; BSA, bovine serum albumin; CC, corpus callosum; EAE, experimental autoimmune encephalomyelitis; ECS, extracellular space; GFAP, glial fibrillary acidic protein; ISM, ion-selective microelectrode; P, postnatal day; PBS, phosphate-buffered saline; SC, superior colliculus; SGS, stratum griseum superficiale; TMA, tetramethylammonium.

pathological states affect ECS diffusion parameters, particularly whether their proliferation and hypertrophy lead to diffusional barriers for neuroactive substances and impaired clearance of metabolites.

To study this issue further, we have used a novel experimental animal model of chronic astrogliosis in CNS tissue. Embryonic cortical or tectal tissue transplanted on to the dorsal surface of the midbrain of neonatal rats matures in the host and develops characteristic cytoarchitectural features.[25,32] In both types of graft, astrocytes are hypertrophied, they stain intensely for glial fibrillary acidic protein (GFAP) and they remain in a reactive state for many months post-transplantation.[22,24] Others have also documented reactive, hypertrophied astrocytes in fetal neural grafts, particularly in grafts that are not well integrated with host tissue.[4,5,26,29,60,69] Oligodendrocytes, in contrast, mature in an apparently normal manner in both tectal and cortical transplants and attain relatively normal phenotypic characteristics.[22,24] In the heterotopic cortical grafts, the increase in astrocytic GFAP immunoreactivity is especially pronounced, and there is an associated increase in chondroitin sulphate proteoglycan expression in the graft neuropil.[22]

Given these findings we decided to study cortical and tectal grafts at different times after transplantation, to investigate whether there are physiologically measurable changes in ECS volume and geometry in grafted tissue. This particular graft model lends itself to such studies because, as the embryonic tissue matures in the host, it grows in volume but remains situated on the dorsal surface of the host midbrain—either on caudal midbrain or on rostral cerebellum.[23,25] The grafts are identifiable as large, discrete tissue masses which are mostly isolated from underlying host tissue, and microelectrodes can be visually guided into the grafted tissue to record neural activity.[21] The location of recording sites can also be verified histologically.[21]

The method used for transplantation of fetal tissue on to the host midbrain involves injection of the tissue through a glass micropipette.[32] This results in a loss of laminar organization; cortical grafts in particular become lobulated, with areas of gray matter separated by irregularly distributed bands or patches of white matter.[22,25] In addition to the influence of astrogliosis, this cytoarchitectural disorganization of the tissue might also affect ECS volume and geometry. To test for this, ECS diffusion parameters were measured in embryonic cortex transplanted on to host cerebral cortex. These homotopic grafts show a similar loss of laminar order, but astrocytic reactivity and GFAP levels are considerably less than in cortex-to-midbrain transplants (Harvey, Kendall and Martins, unpublished observations).

Diffusion in the ECS obeys Fick's laws, subject to two important modifications.[41] First, diffusion in the ECS is constrained by the restricted volume of the tissue available for diffusing particles—by the extracellular volume fraction (α). Second, the free diffusion coefficient, D, is reduced by the square of tortuosity (λ) to an apparent diffusion coefficient $ADC = D/\lambda^2$, because diffusing substances encounter diffusion barriers. These might include cellular membranes, neuronal and glial processes, glycoproteins and macromolecules of the extracellular matrix. α, ADC, λ and non-specific cellular uptake (k') were therefore studied in host cortex and in cortical or tectal grafts, using the real-time iontophoretic method which follows the diffusion of an extracellular marker with ion-selective microelectrodes.[41,62] Recording penetrations were identified histologically and *in vivo* diffusion properties were correlated with morphological features of grafted tissue.

EXPERIMENTAL PROCEDURES

Cortical and tectal tissue grafts

Full details of the transplantation procedure have been given elsewhere.[22,25,32] In short, E15 or E16 embryos (day after mating = E0) were removed from anaesthetized (halothane or ether) time-mated mothers (inbred strain PVG/c for transplantation to the host midbrain and Wistar strain for transplantation to the host cortex; Institute of Experimental Medicine AS CR, Prague). Tectal or cortical tissue was then dissected out and placed in cold Ham's F-10 medium (Gibco-BRL, Gaithersburg, MD, U.S.A.). After removal of overlying membranes, the pieces of tissue were trimmed and then transplanted to the dorsal surface of the midbrain or to the cortex (1–2 mm anterior to lambda) of ether-anaesthetized newborn rats. Transplantation was achieved by slowly injecting the tissue through a glass pipette inserted obliquely under the host skull. After recovery and warming, recipient animals were returned to their mothers; host rats were weaned at 21 days. A total of six host litters received grafts (three litters of cortical grafts, three litters of tectal grafts). In the graft-to-midbrain experiments, to ensure unequivocal identification of the type of graft in host rats, fetal cortex and tectum were transplanted into female and male hosts, respectively. The transplantation of fetal cortical tissue to host cortex was carried out on five male and seven female host rats. All surgical procedures were approved by the appropriate Institutional Ethics Committee. All efforts were made to minimize animal suffering and to reduce the number of animals used.

Electrophysiological studies

At 81–351 days after transplantation, 33 host rats were used in electrophysiological experiments. The weight range was 170–200 g in PVG/c females with fetal cortical tissue transplanted to host midbrain (C-grafts; $n = 18$), 250–300 g in PVG/c males with fetal tectal tissue transplanted to host midbrain (T-grafts; $n = 7$), 300–350 g in Wistar females ($n = 7$) and 500–550 g in Wistar males ($n = 5$), both with fetal cortical tissue transplanted to host cortex (C-C-grafts). PVG/c rats with cortex-to-midbrain grafts were divided into two groups according to the time after transplantation: "young" grafts (81–150-day-old hosts, $n = 13$) and "old" grafts (336–351-day-old hosts, $n = 5$). Control measurements were done in the host cortex of the same animal as graft measurements. The measurements in C-C-grafts were done in 209–245-day-old hosts.

Rats were anaesthetized by injection of 60 mg/kg pentobarbital (i.p.). A state of deep anaesthesia was maintained

throughout each experiment with supplementary injections of pentobarbital (25% of original dose) every 2–3 h. The skin overlying the cranium was removed and the brain surface exposed by cutting the cranial bones with a dental burr and forceps. A craniotomy was performed above the location of the graft, and a second opening was made above the cortical surface of intact host brain. The dura mater was removed above both openings and the head of the animal was fixed in a stereotaxic apparatus. A heating pad was used to maintain body temperature at 37°C. The exposed brain tissue was bathed in warm (37–38°C) artificial cerebrospinal fluid.[31] Electrodes were placed above the brain and penetration was performed using a step-motor microdrive (Nanostepper, SPI, Oppenheim, Germany). Two to five microelectrode tracks were made in each animal, in host cortex and in graft. Measurements were done in *x*- and *y*-axes, the *x*-axis being perpendicular to the body axis and the *y*-axis along the body axis. Diffusion curves were recorded at 200 μm steps between 500 μm and 2300 μm below the transplant surface. Several control measurements in host cerebral cortex were made before, between and/or after the measurements in grafts. The location of the recording sites in transplants was marked by placing a small crystal of the dye DiI on to the surface at the position where the electrodes penetrated the grafted tissue (Fig. 2A). Some electrodes were left in place in the last recording site and fixed *in situ* during the animal perfusion with paraformaldehyde to help to identify the position of the microlectrode penetrations and to facilitate cutting the tissue in the appropriate coronal plane.

Diffusion measurements

Tetramethylammonium (TMA^+)-selective microelectrodes were used to measure diffusion properties of grafts and host cortex. The ion-selective microelectrodes (ISM) for TMA^+ were made from double-barrel tubing as described elsewhere.[64,68] The ion-exchanger was Corning 477317, and the ion-sensing barrel was back-filled with 100 mM TMA chloride while the reference barrel contained 150 mM NaCl. Electrodes were calibrated in a solution of 150 mM NaCl + 3 mM KCl with the addition of TMA^+ at the following concentrations (mM): 0.01, 0.03, 0.1, 0.3, 1, 3, 10. Calibration data were fitted to the Nikolsky equation to determine electrode slope and interference. Iontophoresis pipettes were prepared from theta glass. The shank was bent before back-filling with 0.3 M TMA chloride so that it could be aligned parallel to that of the ISM. Electrode arrays were made by gluing together an iontophoresis pipette and a TMA^+-sensitive electrode with a tip separation of 100–200 μm.

Iontophoresis parameters were + 20 nA bias current (continuously applied to maintain constant electrode transport number) and +80 nA current step of 60 s duration to produce TMA^+ diffusion curves. Potentials recorded at the reference barrel of the ISM were subtracted from ion-selective barrel measurements by means of buffer and subtraction amplifiers. TMA^+ diffusion curves were captured on a digital oscilloscope (Nicolet 310), then transferred to a PC-compatible, 486 computer and analysed by fitting the data to a solution of the diffusion equation by the use of the program VOLTORO (Nicholson, unpublished observations). TMA^+ concentration-versus-time curves were first recorded in 0.3% agar gel (Agar Noble, Difco, Detroit) made up in 150 mM NaCl, 3 mM KCl and 1 mM TMA^+. The iontophoretic curves in agar were used to determine the electrode transport number, *n*, and free TMA^+ diffusion coefficient, *D* (cm^2/s). The diffusion curves were then recorded in the brain and analysed to yield a value of α, TMA^+ apparent diffusion coefficient in tissue *ADC* (cm^2/s), λ ($\lambda = \sqrt{D/ADC}$) and the non-specific TMA^+ uptake, k' (s^{-1}) as previously described.[41,64,65] These parameters were extracted by a non-linear curve fitting simplex algorithm operating on the diffusion curve described by equation (1), which represents the behaviour of TMA^+, assuming that it spreads out with spherical symmetry, when the iontophoresis current is applied for duration *S*.[40,41] In this expression, *C* is the concentration of TMA^+ at time *t* and distance *r*. The equation governing diffusion in brain tissue is:

$C = G(t)$ $t < S$ for the rising phase of the curve
$C = G(t) - G(t - S)$ $t > S$ for the falling phase of the curve.

The function *G(u)* is evaluated by substituting *t* or $t - S$ for *u* in the following equation:

$$G(u) = (Q\lambda^2/8\pi Dar)\{\exp[r\lambda(k'/D)^{1/2}]\mathrm{erfc}[r\lambda/2(Du)^{1/2} + (k'u)^{1/2}] + \exp[-r\lambda(k'/d)^{1/2}\mathrm{erfc}[r\lambda/2(Du)^{1/2} - (k'u)^{1/2}]\}. \quad (1)$$

The quantity of TMA^+ delivered to the tissue per second is $Q = In/zF$, where *I* is the step increase in current applied to the iontophoresis electrode, *n* is the transport number, *z* is the number of charges associated with the substance iontophoresed (+1 here) and *F* is Faraday's electrochemical equivalent. The function "erfc" is the complementary error function. When the experimental medium is agar, by definition, $\alpha = 1 = \lambda$ and $k' = 0$, and the parameters *n* and *D* are extracted by curve fitting. Knowing *n* and *D*, the parameters α, λ and k' can be obtained when the experiment is repeated in the brain.

Diffusion in the cortex is isotropic along the *x*-, *y*- and *z*-axes, while it is anisotropic in the corpus callosum, indicating that diffusion is easier along the myelinated axons (*x*-axis) than across the axons (*y*- and *z*-axes).[11,67] In the case of anisotropic diffusion, we determined α from the relation $\alpha = ((\lambda_y.\lambda_z)/\lambda_x^2)\alpha_x$.[51,67] For this calculation we assume diffusion in the *y*- and *z*- axes to be equal as both axes are at right angles to the direction of the axons.[34]

Immunohistochemistry

Immunohistochemical and morphological studies were undertaken on 37 host rats (19 with C-grafts, 10 with T-grafts, eight with C-C-grafts); about 65% of these animals had previously been used in electrophysiological studies. In all cases, anaesthetized host animals were perfused through the heart with 4% paraformaldehyde in 0.1 M phosphate-buffered saline (PBS; pH 7.5). Brains were postfixed for 4 h, trimmed, immersed in PBS containing 30% sucrose and then encapsulated in egg-yolk.[32] In the rats which had been subject to physiological analysis, the microelectrode that had been left in the grafts at the end of the diffusion measurements was removed prior to immersion in egg yolk.

Frozen coronal sections (40 μm) were cut through the graft and underlying host brain. Sections from grafts containing electrode tracks were first viewed and photographed unstained, to determine the location of the DiI crystals that had been placed on the graft surface at the location of the recording sites. Selected sections were immunostained or stained with Cresyl Violet (Nissl) and Luxol Fast Blue (myelin). Astrocytes were identified using monoclonal antibodies to GFAP (Boehringer-Mannheim, Mannheim, Germany), while oligodendrocytes and myelin were immunostained with Rip, a monoclonal antibody specific for oligodendroglia and central myelin.[15] GFAP antibodies were diluted 1:20 in Dulbecco's "A" PBS solution containing 1% bovine serum albumin (BSA, Sigma, Prague, Czech Republic) and 0.2% Triton X-100; the Rip supernatant (courtesy of Dr B. Friedman, University of Iowa, U.S.A.) was used neat, with 1% BSA and 0.2% Triton X-100 added. After overnight incubation in the primary antibodies at 4°C, the floating sections were washed and processed using biotinylated anti-mouse secondary

antibodies and the avidin–biotin peroxidase complex method (Vectastain Elite, Vector Laboratories, Burlingame, CA, U.S.A.). Immune complexes were visualized using 0.05% 3,3′-diaminobenzidine tetrachloride (Sigma) in 0.05 M Tris buffer (pH 7.6) and 0.02% H_2O_2. Sections were mounted on gelatin-coated glass slides, dehydrated and coverslipped.

Statistical analysis

The statistical significance of data from grafted tissue and host cortex was evaluated by one-way ANOVA. Significance was accepted when $P < 0.05$. All data are expressed as mean ± S.E.M.

RESULTS

Morphological characteristics of the grafts—immunohistochemistry

The glial organization and myeloarchitecture of C- and T-grafts were similar to that described previously.[22,24] Examples of Rip immunostaining of a C-graft and a T-graft three to four months post-transplantation are shown in Fig. 1A and B, respectively. Both grafts were located on the host midbrain, but the pattern of Rip immunoreactivity in the two types of transplant was markedly different. C-grafts were usually 2.0–2.5 mm thick, and most of the grafts consisted of gray matter areas containing loosely packed neurons separated into lobules by irregularly organized white matter-like patches or bundles (arrow in Fig. 1A; Fig. 2B, C). T-grafts were generally smaller (1.0–1.5 mm thick) and, in contrast to C-grafts, consisted mainly of neurons intermixed with dense networks of myelinated (Rip-positive) fibres (Fig. 1B). They contained a small number of highly localized regions that possessed little or no Rip immunoreactivity (arrows in Fig. 1B). The patterns of Rip immunostaining in cortical and tectal transplants reflected the origin of the two types of tissue. Note in Fig. 1B that most of the host cerebral cortical volume comprises gray matter, whereas in the host superior colliculus (SC) only one of the seven tectal laminae—the superficial layer (SGS, stratum griseum superficiale)—is truly gray matter-like in appearance.

C- and T-grafts typically revealed increased GFAP immunoreactivity compared with host neocortex and host SC, respectively (cf. Refs 20, 22 and 24). The level of staining in young C-grafts was particularly high, there being increased GFAP immunoreactivity throughout much of the graft neuropil (Figs 1C, 2E). Astrocytes were hypertrophied (Fig. 1D) compared with astrocytes in host cortex (Fig. 1E). A consistent finding in these grafts was a decrease in the density of astrocytes in the localized white matter-like regions (arrow in Fig. 1C; Fig. 2E, F). Compared with young grafts, in old C-grafts there was a clear decrease in GFAP immunoreactivity throughout the grafted tissue (Fig. 1F, G). However, astrocytes were still hypertrophied compared with cells in similarly aged host cortex (compare Fig. 1G with Fig. 1H). Rip-positive bands of white matter were also evident (data not shown) and, as in young grafts, there were fewer astrocytes in these regions (arrow in Fig. 1F).

Some of the C-C-grafts (1.5–2.0 mm thick) were well integrated within the host cortex, compared with grafts transplanted to the midbrain, and consisted mostly of gray matter areas (Fig. 3A). Others were not incorporated into the cortex, were separated by a densely stained GFAP border from the host cortex (Fig. 3C) and contained gray matter as well as irregularly organized bundles of white matter. The C-C-grafts also possessed increased GFAP immunoreactivity. In well-integrated C-C-grafts the astrocytic reactivity was less prominent than in C- and T-grafts (Fig. 3A). In those cases in which the C-C-grafts were not well incorporated within the host cortex, they exhibited more intense staining for GFAP (Fig. 3C).

Diffusion parameters in host cortex and corpus callosum

In all experiments the extracellular space diffusion parameters—the extracellular space volume fraction α, tortuosity λ and non-specific TMA^+-uptake k'—were studied in all cortical layers and in the corpus callosum (CC) of host brain. In addition, measurements were performed in nine control

Fig. 1. Immunohistochemistry and morphology of a cortex-to-midbrain and tectum-to-midbrain graft. (A) A coronal section of host brain with a cortical graft (T) immunostained for Rip (three months post-transplantation). Note the localized white matter-like band of myelinated axons (arrows) in the middle of the graft. (B) A coronal section of host brain with a tectal graft (T) immunostained for Rip (four months post-transplantation). The bulk of the graft contained a dense network of myelinated axons; note the occasional localized area containing little or no Rip immunoreactivity (arrows). (C–E) Cortical graft and host cortex examined in an animal three months post-transplantation—GFAP immunohistochemistry. (C) Low-power view of cortical graft, showing the intense GFAP immunostaining typical of most parts of the graft. Localized white matter-like regions contained fewer astrocytes (arrow). The area outlined by the box is shown at higher power in D. In D, note the hypertrophied appearance of the astrocytes and the dense network of $GFAP^+$ processes. (E) $GFAP^+$ astrocytes in the gray matter of host cortex. (F–H) Cortical graft and host cortex examined in an animal 10 months post-transplantation—GFAP immunohistochemistry. (F) Low-power view of graft. A white matter-like region is arrowed. This old graft contains less GFAP immunoreactivity than is seen in younger transplants. The boxed area in F is shown at higher power in G. (H) $GFAP^+$ astrocytes in the gray matter of host cortex. Cx, host cortex; sgs, stratum griseum superficiale of host superior colliculus; bv, blood vessel. Scale bars: (A, B) = 1 mm; (C, F) = 200 μm; (D, E, G, H) = 40 μm.

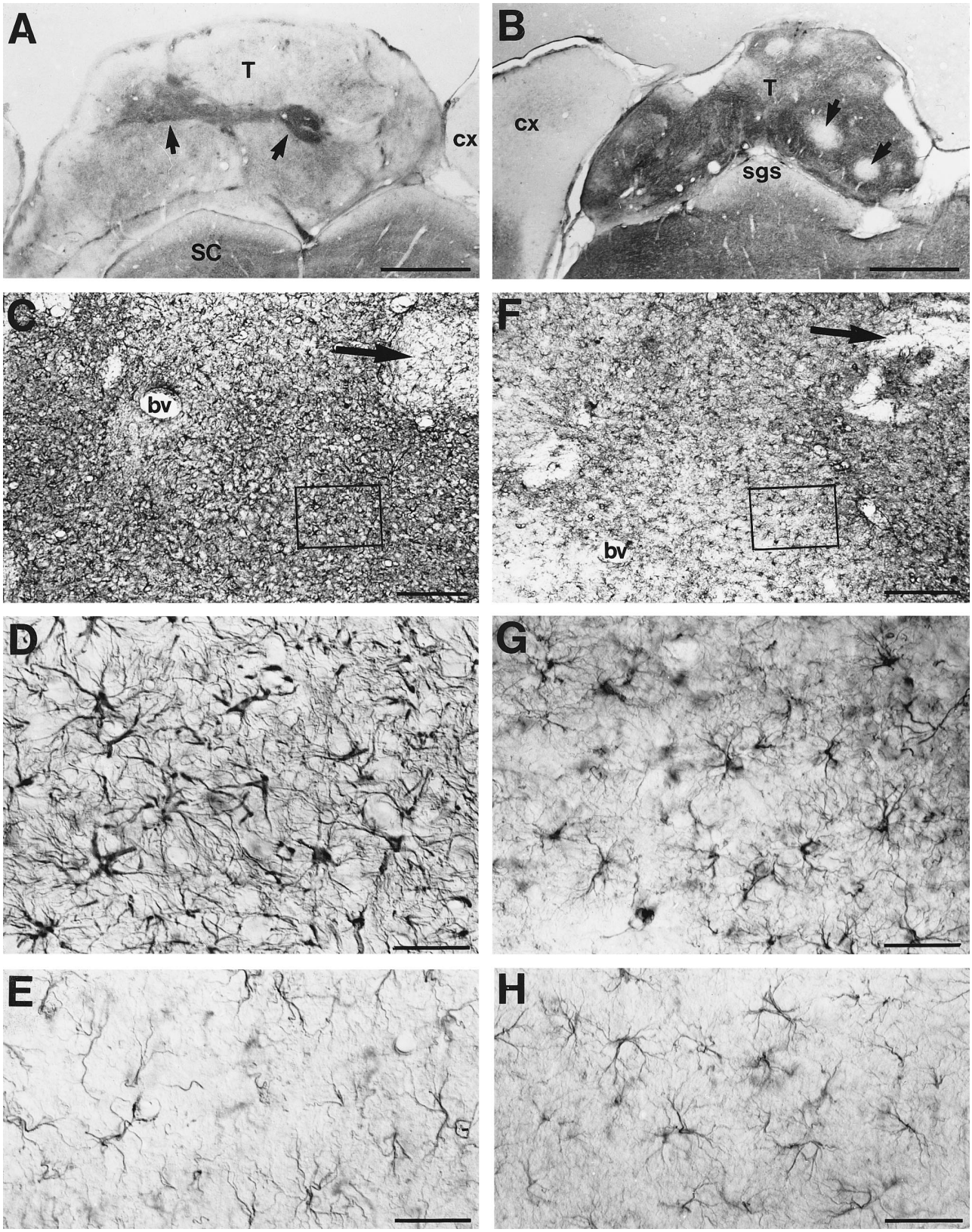

Fig. 1.

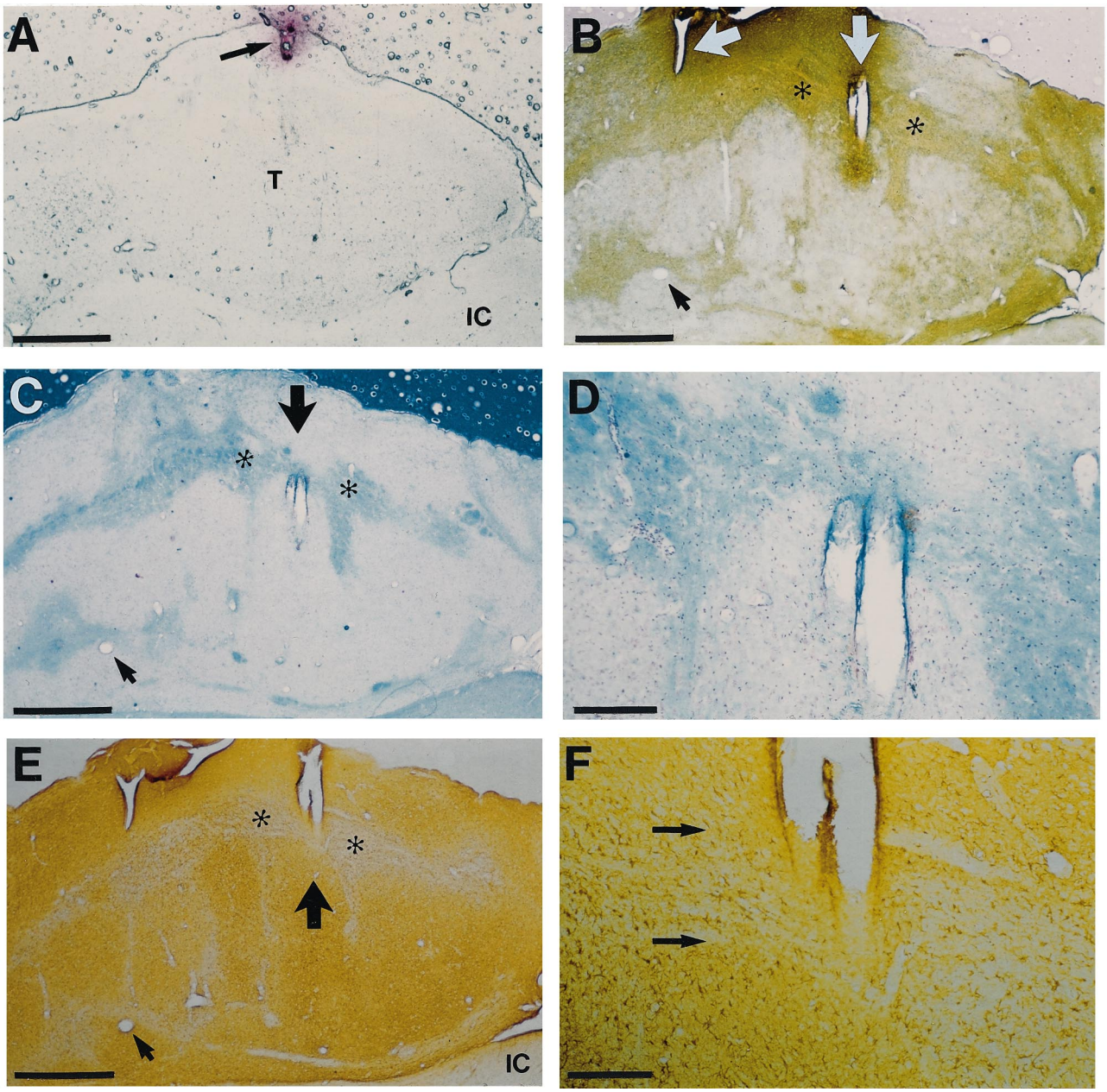

Fig. 2. Colour photomicrographs showing histological identification of two electrode tracks in a young cortex-to-midbrain graft (T) (three months post-transplantation). (A) Unstained section showing DiI crystal (arrow) at the site of electrode penetration. (B) Coronal section immunostained for Rip showing two electrode tracks (large white arrows; track 1 to the left, track 2 to the right). Both tracks passed through a band of Rip^+ white matter (asterisks). (C, D) Section stained with Luxol Fast Blue and Cresyl Violet. (C) Track 2 (large arrow) is visible passing through the white matter-like band (asterisks). (D) Higher power view of electrode track. (E, F) Section adjacent to that shown in B, immunostained for GFAP. Note tracks 1 and 2. (E) Track 2 (large arrow) passed through a band containing a low density of astrocytes (asterisks) which corresponded to the Rip^+ band shown in B. (F) Higher power view of track 2. Arrows delineate the band containing fewer $GFAP^+$ astrocytes. For orientation, a blood vessel common to all sections is denoted by the small arrow in B, C and E. IC, host inferior colliculus. Scale bars: (A, B, C, E) = 1 mm; (D, F) = 200 μm.

animals from the same litters which had no grafted tissue. No significant differences were found between the cortex and CC of control animals (i.e. without grafts) and graft recipients. In cortical layers III–VI, the mean α ranged from 0.20 to 0.21 and λ from 1.59 to 1.64 (see Table 1, Fig. 4). As we reported previously,[34,67] the diffusion in cortical gray matter was isotropic; that is, the values of λ were not found to be significantly different between the *x*-, *y*- and *z*- axes. The value of α found in CC white matter was about the same as that found in gray matter; however, the diffusion was anisotropic

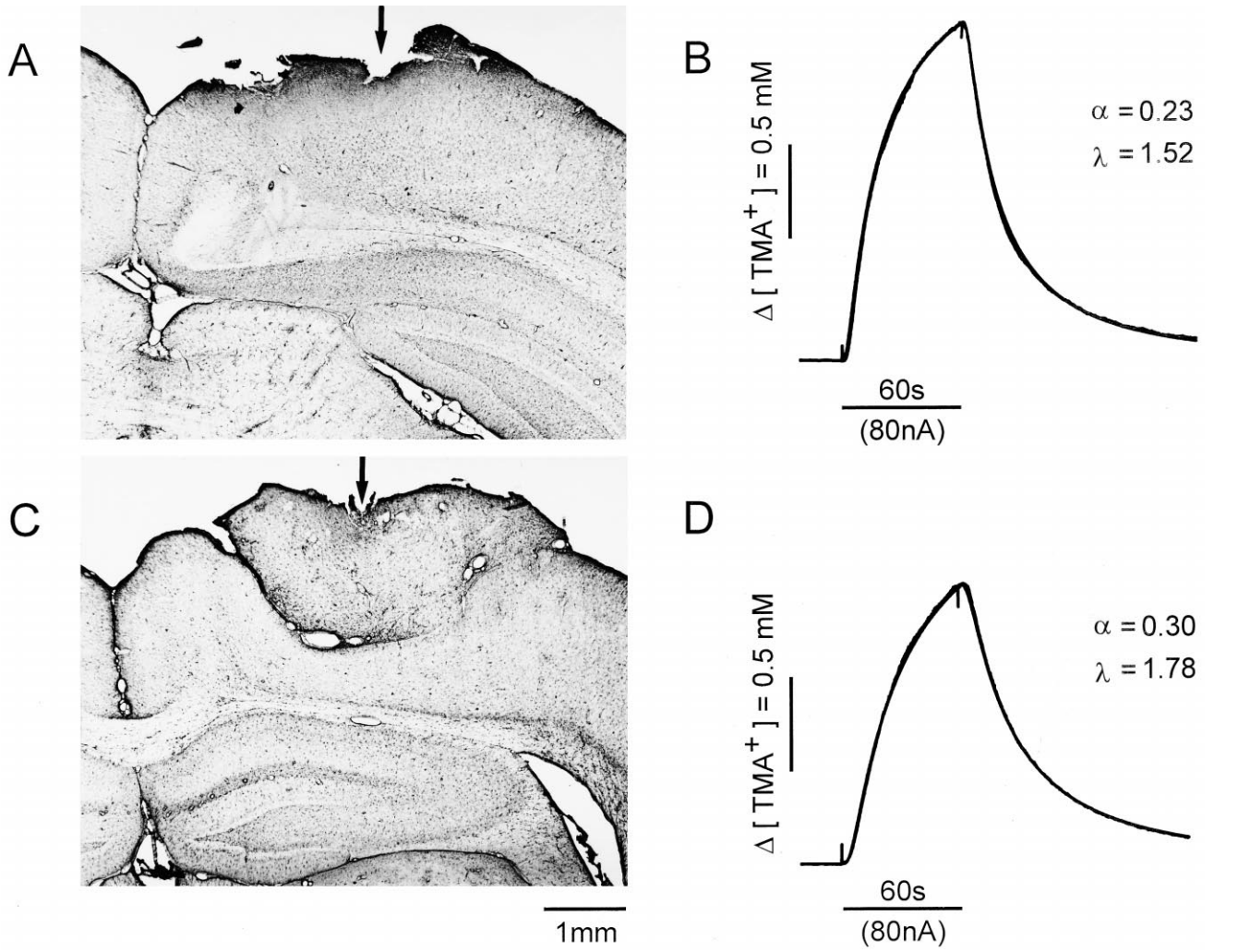

Fig. 3. Photomicrographs showing two cases of the integration of fetal cortical tissue within the host cortex (GFAP staining). (A) Well-integrated transplant (209 days post-grafting) and (C) poorly integrated transplant (231 days post-grafting) with identified electrode tracks (arrows). Note the more intense GFAP immunoreactivity in the transplant in C. The representative curves (B and D) recorded in this experiment and the respective α and λ values demonstrate the differences in diffusion properties of well-integrated (B) and poorly integrated (D) transplants.

with mean values of $\lambda_x = 1.41 \pm 0.02$ along the axons, $\lambda_y = 1.74 \pm 0.03$ and $\lambda_z = 1.75 \pm 0.04$ across the axons (Table 1). The quantile plots in Fig. 5 simply place all data in order of ascending value and then plot the value against the rank order (expressed as a number between 0 and 1). In the case of the anisotropic diffusion in host CC, the λ_x values were smaller than the λ_y and λ_z values, i.e. the values fell into two groups, lower values being found along the axons and higher ones across the axons.

Diffusion parameters in young cortex-to-midbrain and tectum-to-midbrain grafts

Following control diffusion measurements made in host cortex and CC, measurements were performed in the respective grafts. Figure 4 shows typical diffusion curves recorded in host cortex and in the C-graft of the same animal. The values of α and λ were substantially higher in both young cortical (Fig. 6) and tectal grafts than in host cortex. In young C-grafts [postnatal day (P) 81–P135] the mean value of α was 0.34 and of λ 1.78 (Table 1). In young T-grafts (P105–P150) the mean value of α was 0.29 and of λ 1.85. Thus, both parameters were significantly higher than those in host cortex at any location in the graft neuropil. The mean non-specific cellular uptake k' in young cortical and tectal grafts was significantly higher than that in host cortex or CC (Table 1). The λ values were generally larger in T-grafts, which contained more white matter, than in C-grafts containing more gray matter. This corresponds to the higher values of λ seen in CC than in host cortex when measured across the axons.

About 50% of the microelectrode penetrations

Table 1. Extracellular space diffusion parameters in host cortex, host corpus callosum, fetal cortical tissue transplanted to host midbrain (81–135-day-old "young" C-grafts and 336–351-day-old "old" C-grafts), fetal tectal tissue transplanted to host midbrain (105–150-day-old T-grafts) and fetal cortical tissue transplanted to host cortex (209–245-day-old C-C-grafts)

		n	*N*	α	λ	k' (10^{-3}/s)
Host cortex	layer III	15	13	0.21 ± 0.01	1.64 ± 0.02	3.54 ± 0.69
	layer IV		18	0.21 ± 0.01	1.62 ± 0.02	3.28 ± 0.66
	layer V		37	0.20 ± 0.01	1.60 ± 0.02	3.49 ± 0.44
	layer VI		19	0.21 ± 0.01	1.59 ± 0.01	3.41 ± 0.27
Host corpus callosum	*x*-axis	9	20		1.41 ± 0.02	
	y-axis		8	0.21 ± 0.01	1.74 ± 0.03	2.75 ± 0.36
	z-axis		9		1.75 ± 0.04	
Young C-grafts		13	115	0.34 ± 0.01[b]	1.78 ± 0.03[b]	4.35 ± 0.22[a]
Old C-grafts		5	85	0.27 ± 0.01[b]	1.57 ± 0.01	2.96 ± 0.28
Young T-grafts		7	15	0.29 ± 0.02[b]	1.85 ± 0.04[b]	7.23 ± 0.71[b]
C-C-grafts		8	66	0.24 ± 0.01[a]	1.66 ± 0.02[a]	4.16 ± 0.21[a]

α, ECS volume fraction; λ, ECS tortuosity; k', non-specific uptake; *n*, number of animals; *N*, number of measurements. Data are expressed as mean ± S.E.M.
a: significant difference ($P < 0.05$) between host cortex (layers V and VI) and respective group. b: significant difference ($P < 0.0005$) between host cortex (layers V and VI) and respective group.

through grafted tissue were identified in histological sections, and comparisons were made between diffusion parameters and morphological data. An example of such an analysis is presented in Figs 2 and 6, which show coronal sections of the cortex-to-midbrain graft and the values of diffusion parameters measured in host cortex and grafted tissue from the same animal. Two identified tracks were recorded by the same microelectrode array. Figure 2 shows that the first penetration of the microelectrode (track 1) crossed a gray matter area, passed through a white matter bundle and finished at a depth of about 1700 μm in gray matter. Track 2 can be seen passing again through gray matter, then reaching a region of white matter at a depth of about 900 μm and finishing at a depth of 1500 μm inside gray matter (Fig. 2). The extracellular space diffusion parameters measured in any grafted tissue were heterogeneous, in contrast to the typical homogeneity found in host cortex, and the highest values of λ were found in white matter bundles, in track 1 at 1100 μm and in track 2 at 900 μm and 1100 μm (Fig. 6).

Diffusion heterogeneity of grafted tissue

A comparison of the two-dimensional pattern of diffusion away from a point source in a graft is shown in Fig. 7. Figure 7 shows the diffusion curves recorded in three microelectrode tracks in the same C-graft separated by 500 μm in the *y*-axis and aligned in parallel in the *x*-axis. The diffusion curves were measured at various depths from the graft surface. The values of α, λ and k' from these curves were used to construct isoconcentration circles in the *x*–*y* plane (note that only a single value of λ has been obtained at each measurement site). The circles show the concentration of TMA^+ (0.1–1.0 mM), calculated after 60 s of iontophoretic application in the graft. The plots show the diffusion pattern in various regions of the graft and illustrate the differing ability of particles to diffuse in different regions of the grafted tissue.

Diffusion anisotropy of grafted tissue

Figure 5 shows the distribution of all measured values of α and λ as described by quantile plots of the data.[10,51] These plots demonstrate that higher and more distinct values of α and λ were found in grafted tissue than in host cortex and CC, suggesting anisotropy in grafted tissue. Figure 7 shows that there is a great heterogeneity in grafted tissue, even between areas not more than 200 μm apart. To test for anisotropy, we made two or three tracks in the same area and depth of grafted tissue; in one track the alignment of the iontophoretic and ion-selective electrodes was perpendicular to the body axis (*x*-axis), whereas in the second track they were aligned along the body axis (*y*-axis). In these experiments the values of λ_x and λ_y in a graft always differed regardless of depth, suggesting that the diffusion in grafts is largely anisotropic (Fig. 8). The same values of α, λ and k' as given in Fig. 8 were used to construct isoconcentration plots in the *x*–*y* plane representing diffusion in host cortex and in the graft. When the tortuosity is increased along one of the axes, e.g., across the fibres, the isoconcentration plot is represented by an ellipse. The ellipse in Fig. 8 illustrates the concentration of TMA^+ (0.1–1.0 mM), calculated after 60 s of iontophoretic application in the graft. In addition, the ellipse for the graft is much smaller than the circle for host cortex, owing to the larger ECS volume fraction.

Diffusion parameters in old cortex-to-midbrain grafts

In old C-grafts (P336–P351) the mean α value was 0.27 and the mean λ value 1.57. Although the

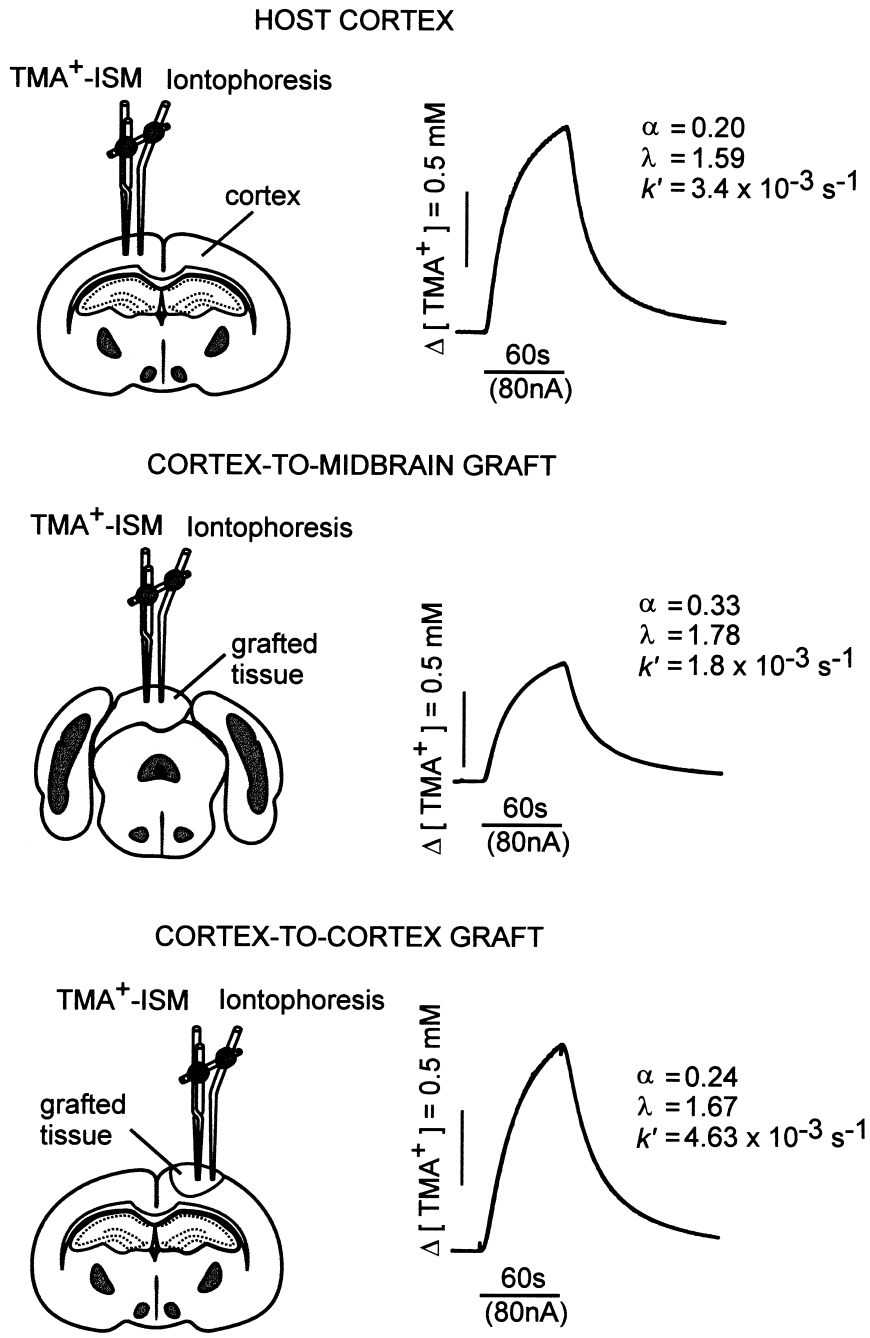

Fig. 4. Experimental arrangement and TMA^+ diffusion curves obtained from host cortex, cortex-to-midbrain graft (135 days post-transplantation) and cortex-to-cortex graft (231 days post-transplantation). The concentration scale is linear, and the theoretical diffusion curve is superimposed on each data curve. Recordings in host cortex and young cortex-to-midbrain graft were made in the same animal using the same microelectrode array. The measurements in host cortex and in graft were performed at the same depth of 700 μm; the separation between the ion-selective microelectrode and iontophoresis electrode tips was 119 μm; the iontophoretic electrode transport number $n = 0.303$. The measurements in cortex-to-cortex graft were performed at a depth of 900 μm; the electrode tip separation was 156 μm; the iontophoretic electrode transport number $n = 0.430$.

mean α was still significantly higher than in host cortex, it was significantly lower than in young grafts. No significant difference was found between the mean λ values in old grafts and host cortex lamina V and VI (Table 1). It is worth reiterating here that there was substantially decreased GFAP staining in these older grafts compared with young grafts (Fig. 1). In addition, in old cortical grafts the uptake was not significantly higher than that in host cortex or CC, suggesting that hypertrophied and proliferative astrocytes could be responsible for k' increase.

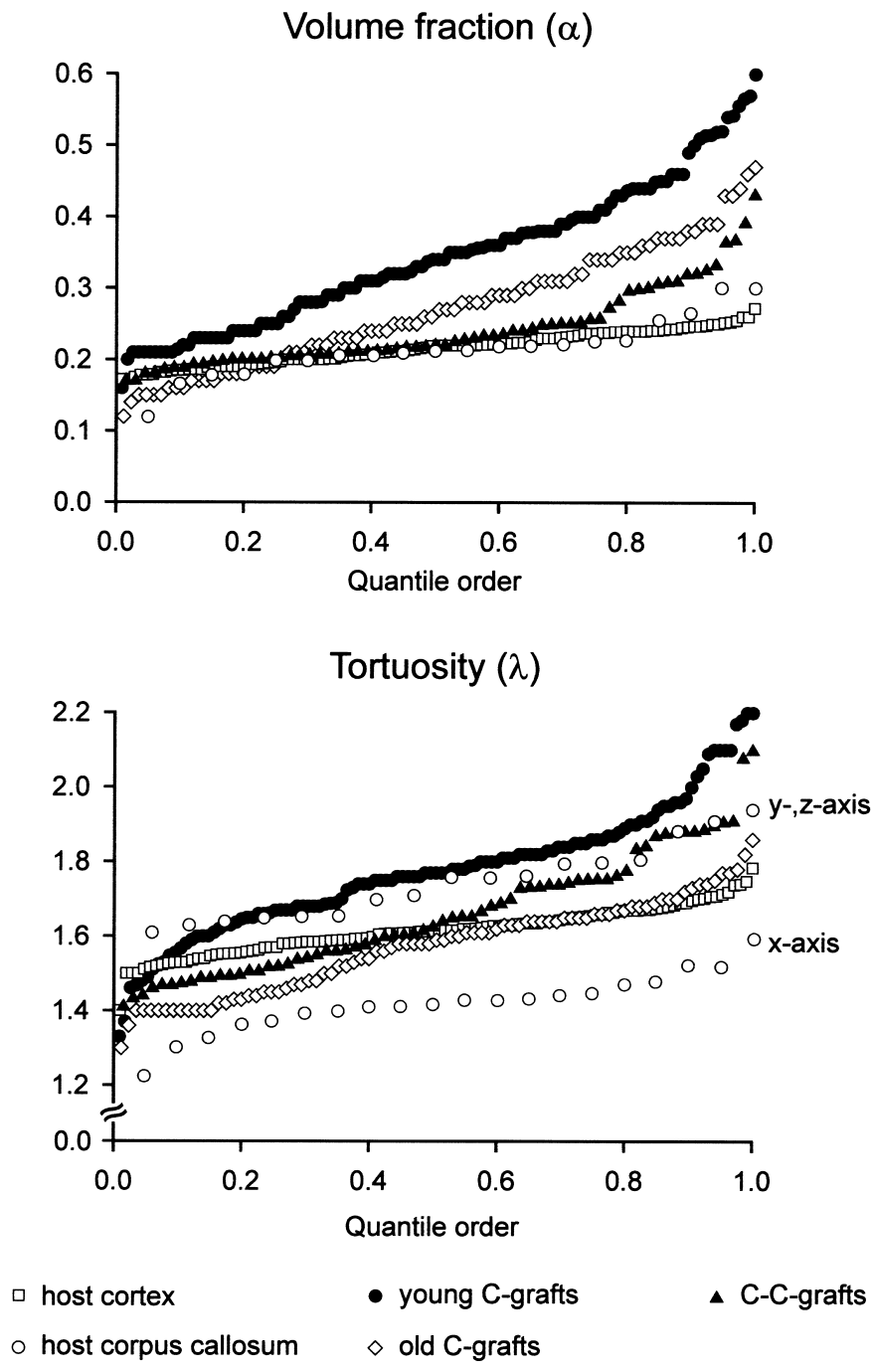

Fig. 5. Quantile plots of α and λ values in host cortex, young and old cortex-to-midbrain grafts (young and old C-grafts), cortex-to-cortex grafts (C-C-grafts) and host corpus callosum (host CC). All data for each group were plotted in order of ascending value and then each value was plotted against its rank as a fraction of the number of observations in the appropriate group. In host CC, λ values were recorded from the *x*-, *y*- and *z*-planes. Note the similarity of median values of α in host cortex, host corpus callosum and C-C-grafts. Median values of λ were similar in old C-grafts, host cortex and C-C-grafts. Also similar were the median values of λ in young C-grafts and host corpus callosum (along *y*-, *z*-axis). Sample size varied among groups (see Table 1 for *n* and for calculated mean ± S.E.M.).

Diffusion parameters in cortex-to-cortex grafts

In cortical tissue grafted to host cortex the mean values of α and λ (0.24 and 1.66, respectively) were still significantly higher than those in host cortex (Table 1). However, these values were significantly lower than those in young C-grafts. Similar to young cortical grafts, k' was significantly higher than in host cortex. In some cases in which the fetal cortical tissue was not well incorporated within the host

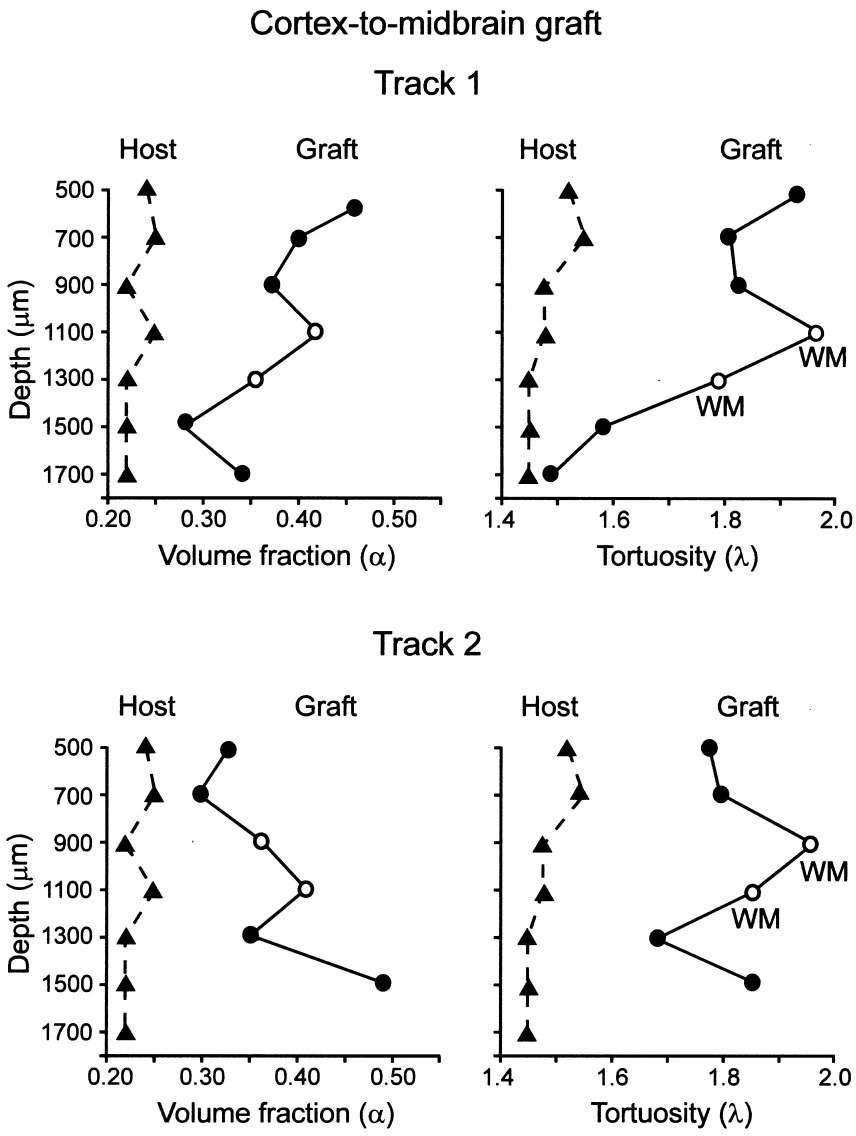

Fig. 6. Diffusion parameters recorded at various depths in host cortex and in two microelectrode tracks in a young cortical graft. The graphs show the values of volume fraction (α) and tortuosity (λ) obtained in one animal with a cortical graft (three-month-old). For immunohistochemistry and location of the tracks see Fig. 2, in which both tracks are localized in the same animal. The same microelectrode array was used to record diffusion curves in host cortex (host, filled triangles) and in two tracks in cortical graft (graft, dots and circles). The circles represent data from identified white matter bundles (WM).

brain tissue, the values of volume fraction and tortuosity were consistently higher than the mean values in these grafts. Figure 3 shows integrated (A) and poorly integrated (C) C-C transplants with identified electrode tracks. In poorly integrated grafts, GFAP expression was more prominent and α and λ values were significantly higher (Fig. 3C, D) than in integrated grafts (Fig. 3A, B).

DISCUSSION

Our data represent the first characterization of the diffusion properties and ECS characteristics of fetal brain transplants. *In vivo* measurements in mature cortical and tectal grafts to the midbrain (C- and T-grafts) as well as in non-incorporated cortex-to-cortex (C-C) grafts showed significantly larger values of α (ECS volume fraction) and λ (tortuosity) compared with host brain. While diffusion in the host cortex was largely homogeneous and isotropic, in grafts diffusion was anisotropic and heterogeneous. Different values of α and λ correlated with morphological heterogeneity in the graft neuropil. All grafts lacked the laminar organization typical of normal neocortex and SC; however, C-C-grafts that were well incorporated into the host cortex had α and λ values close to those found in host cortex (see Figs 3A, B, 4).

The values of α in C- and T-grafts in particular were as high as in the cortex of two to five-day-old

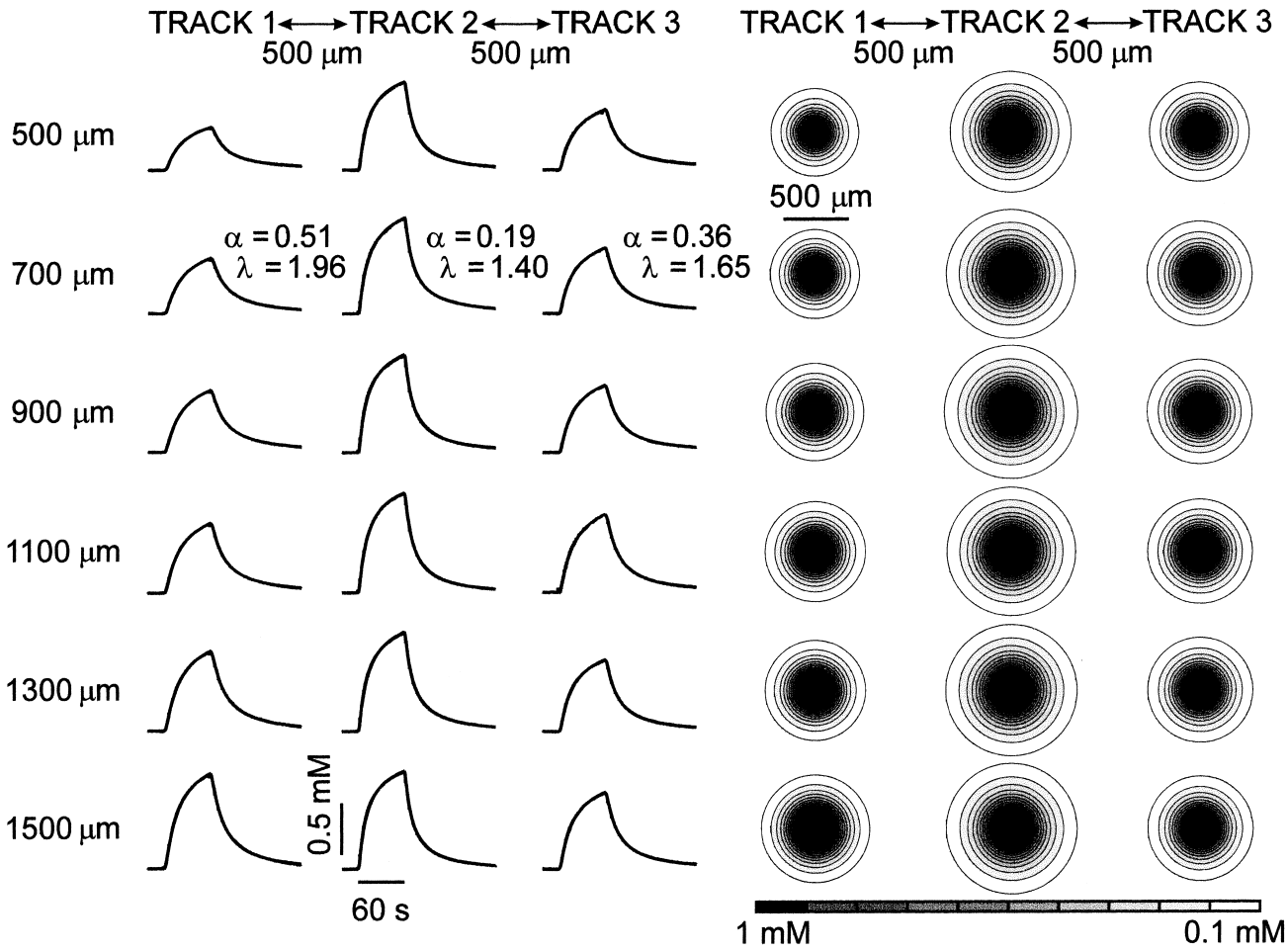

Fig. 7. Diffusion in grafted tissue. (Left) Diffusion curves obtained at different depths in three different tracks in a young cortex-to-midbrain graft (127-day-old). The respective α and λ values are only shown with the three representative curves from a depth of 700 μm. Distance between the three tracks was about 500 μm. All diffusion curves were recorded with the same microelectrode array: electrode spacing $r = 122$ μm, electrode transport number $n = 0.354$. (Right) Two-dimensional isoconcentration plots of TMA^+ concentration in different graft regions after 60 s of iontophoretic application of TMA^+. Gray densities represent different concentrations of TMA^+ from 0.1 to 1.0 mM. Isoconcentration plots were calculated using diffusion parameters obtained from the corresponding diffusion curves on the left. The iontophoretic pipette served as a point source of TMA^+. The larger the circle, the more restricted the diffusion of TMA^+ in that region of the graft.

rats,[31,68] suggesting that these transplants may have retained some of the diffusion characteristics of immature brain. Based on a number of immunocytochemical studies, Rosenstein[53,54] has also suggested that cortical grafts may possess an immature structure and metabolism (cf. Ref. 18). Electron-microscopic studies have revealed that developing nervous tissue has a larger ECS[6,49] and greater abundance of extracellular glycosaminoglycans and hyaluronate than adult tissue.[33] In previous diffusion studies we found the ECS to be twice as large in immature tissue as in adult brain, but the values of λ tended to be significantly lower ($\lambda \approx 1.5$).[31,68] This suggests that the observed increase in tortuosity in fetal cortex and tectal grafts is due to factors different from those normally present in the developing brain.

Anisotropy has not been found in the gray matter of either host cerebral cortex or developing cortex.[34,67] In corpus callosum white matter, significant anisotropy exists only after myelination.[48,67] Our present experiments show that λ in grafted tissue is increased in gliotic gray matter and is even higher in white matter-like regions, suggesting that diffusion of neuroactive substances in white matter bundles is less efficient than in gray matter. This is apparently because diffusion is more hindered across the fibres than along the fibres.[3,67] Myelinated bundles are present in many regions of the graft with no preferential orientation towards any one axis.

To completely analyse the behaviour of small molecules, TMA^+ diffusion measurements must be carried out in two or three dimensions. In the present experiments, measurements were made in the same animal and in the same area of the graft in two

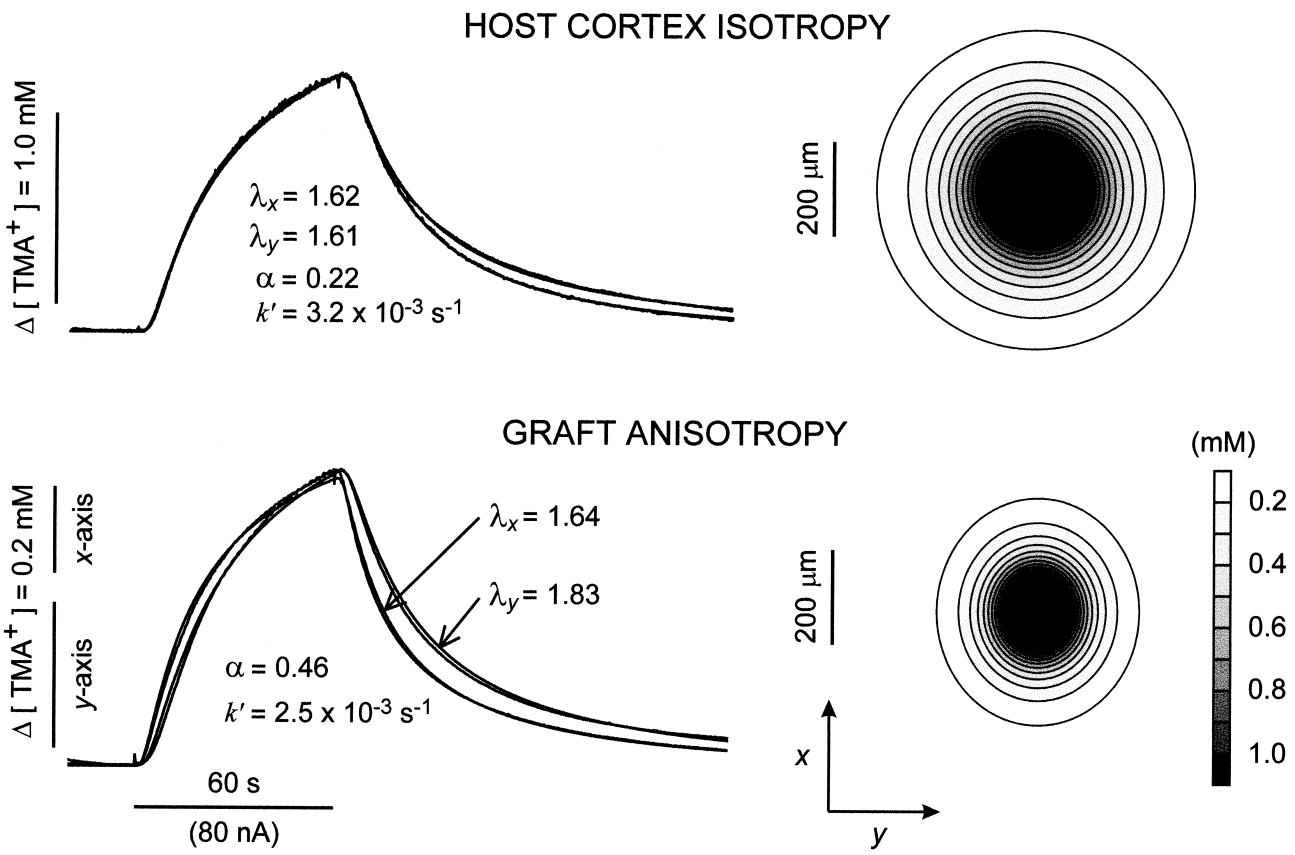

Fig. 8. Representative diffusion curves recorded in a host cortex and in a young C-graft (82 days post-transplantation) in the *x*-axis (perpendicular to the body axis) and in the *y*-axis (along the body axis) with the same microelectrode array. Recordings in *x*- and *y*-axis are from the same animal, region and depth in host cortex (900 μm) and in the graft (700 μm). Note the different time-course of the diffusion curves in the graft due to the different values of λ, showing the substantial anisotropy of the grafted tissue. Two-dimensional isoconcentration plots of TMA^+ concentration in different graft regions after 60 s of iontophoretic application of TMA^+. Gray densities represent different concentrations of TMA^+ from 0.1 to 1.0 mM. Isoconcentration plots were calculated using diffusion parameters obtained from the corresponding diffusion curves shown in this figure. The iontophoretic pipette served as a point source of TMA^+. Note that the diffusion in host cortex is represented by a circle (diffusion is isotropic), while that in the graft is represented by an ellipse due to diffusion anisotropy.

dimensions, along and across the body axis. The λ values associated with the two microelectrode orientations were indeed different, showing anisotropic diffusion (see Figs 5, 8). Because of different values of λ, the calculation of α values from a set of measurements made exclusively in one axis will be subject to systematic error.[51] However, because there is no preferential organization of fibre tracts in any one direction in grafted tissue, the mean λ and α values given in Table 1 represent average values in all three directions. Clearly, the α values measured in any direction and place in grafted tissue were significantly higher than those in host cerebral cortex.

Recently, a large ECS volume fraction was described in the spinal cord of rats with experimental autoimmune encephalomyelitis (EAE).[57] Vasogenic edema, inflammatory reaction and blood–brain barrier (BBB) damage in EAE rats result in a dramatic increase in ECS volume fraction, which is, however, accompanied by a decrease in tortuosity. Since we have observed an increase in microglial cell reactivity in C- and T-grafts,[20,22] we cannot exclude the presence of a low-level inflammatory reaction and some abnormalities in the BBB in tissue transplanted to the neonatal midbrain. Although there is evidence for an intact BBB in fetal cortical tissue grafted to cortex,[61] it has also been reported that angiogenesis in cortical grafts varies depending on the site of transplantation.[13] Astrocytes are involved in BBB formation,[27] and the reactive astrocytes seen in cortical grafts[22] and around blood vessels in grafts[30] might have some impact on the status of the BBB. Indeed, it has been suggested that fetal cortical grafts may be subject to a sublethal form of ischemic injury.[54] Low-level inflammation and changes in the BBB could contribute to extracellular accumulation of fluid and an increase in α; however, they cannot explain the observed increase in tortuosity which is the cause of lower diffusibility in grafted tissue.

In “old” C-grafts (336–351-day-old hosts), the volume fraction α was lower than in “young”

C-grafts (81–135-day-old hosts) but still higher than in host cortex. The average tortuosity in old grafts decreased to the range of host tissue; however, higher λ values were observed in small patches of grafted tissue and diffusion remained heterogeneous and anisotropic. Importantly, along with a decrease in λ, there was a marked decrease in GFAP immunoreactivity. This suggests that astrogliosis may be an important cause of the observed high tortuosity values and decreased diffusibility in transplanted tissue. Consistent with this, C-C-grafts that were well integrated with host cortex possessed only minimal astrocyte reactivity and had λ and α values similar to the host; non-incorporated C-C-grafts had higher levels of GFAP immunoreactivity and higher λ and α values.

There are two possible explanations for the observed increase in tortuosity in gliotic grafts. First, reactive astrogliosis is characterized by an increase in the thickness, length and presumably also number of glial processes,[5,22,26] and these can form diffusion barriers between cells. Second, reactive astrocytes produce a variety of extracellular matrix molecules such as sulphated proteoglycans, tenascin and vitronectin.[14,35,36,43,59] Increased expression of different types of extracellular matrix may hinder the diffusion of other particles in grafts[47,66] and may also push cells apart, hence increasing values of α. In this regard, increased levels of chondroitin-6-sulphate proteoglycan immunoreactivity have been found in C-grafts,[22] and we recently reported increased λ values in spinal cord superfused with dextran and hyaluronate.[47] Together, these observations suggest that much of the observed increase in tortuosity in grafts may be due to an increased content of macromolecules in the ECS (e.g., extracellular matrix molecules).

Many of the macromolecules produced by activated astrocytes can influence neuronal maturation and axonal growth. Changes in astrocytic phenotype may also affect the formation and stability of synapses,[37,38,45] and it is of interest that in fetal cortical tissue grafted to the striatum, there is continuous up-regulation of the synaptosomal-associated protein SNAP-25,[55] believed to play a role in neural plasticity.[7] Given the chronic gliosis in C-, T- and some C-C-grafts and the accompanying changes in ECS diffusion parameters described in the present study, changes might also be expected in the glial control of ionic homeostasis[28,62] and in synaptic and extrasynaptic transmission in the graft neuropil.[1,16,42,62]

There have been numerous studies examining the electrophysiological characteristics of fetal grafts and the extent to which host synapses are effective in activating neurons in fetal tissue.[2,8,9,17,19,21,39,56] Most of these authors have highlighted the similarities between neuronal activity in grafts and normal host tissue; however, there have been occasional reports describing abnormal electrophysiological activity in grafts. For example, Siviy *et al.*[58] reported high-amplitude, long-duration depolarizing synaptic potentials in neostriatal grafts, suggesting that neurons became hyperexcitable to glutaminergic synaptic input. Isolated cortical grafts *in oculo*, which develop a substantial gliosis,[4] also possess a number of abnormal electrophysiological characteristics.[44] Of particular relevance to the present work is a study in which fetal tectal tissue was transplanted on to the midbrain of neonatal rats and single units were recorded in transplants in mature hosts.[21] Action potentials recorded from transplant units were relatively small in amplitude and, compared with underlying host tissue, less readily isolated from the background activity. These differences in electrical characteristics were hypothesized to be related to changes in the resistivity of grafted tissue.[21]

CONCLUSIONS

Fetal cortical grafts are a useful model in which to study how chronic, global glial cell reactivity can affect the physiological properties of CNS tissue. In addition, we believe it is of value to determine whether the apparent association between astrocyte reactivity and changes in ECS diffusion parameters described here in grafted neural tissue also holds for other neuropathological conditions associated with gliosis. It is known, for example, that extracellular matrix molecules are produced and released by astrocytes and are a feature of the glial reaction accompanying traumatic injury,[14,35] epilepsy[43] and human neurodegenerative disorders such as Alzheimer's disease.[12,14,46] Importantly, an increase in λ has indeed been observed in gliotic tissue after experimental irradiation injury[65] or after cortical stab wounds.[52] Such changes in ECS tortuosity and/or volume may constrain or affect the diffusion of a variety of neuroactive substances, including ions, neurotransmitters, cytokines, enzymes and neurotrophic factors. This, in turn, may impact upon neuronal viability, function and synaptic and extrasynaptic transmission in the affected CNS tissue.

Acknowledgements—Supported by grants GACR 309/96/0884, GACR 307/96/K226, IGA MZ 3423-3, VS 96-130 to ES, and an NHMRC grant to ARH. Thanks to Margaret Pollett and Natalie Symons for assistance in the preparation of histological material.

REFERENCES

1. Agnati L. F., Zoli M., Stromberg I. and Fuxe K. (1995) Intercellular communication in the brain: wiring versus volume transmission. *Neuroscience* **69,** 711–726.

2. Bassant M. H., Joly M., Nilsson O. G., Björklund A. and Lamour Y. (1988) Electrophysiological and pharmacological properties of neurons with solid basal forebrain transplants in the rat brain. *Brain Res.* **460,** 8–16.
3. Bjelke B., England R., Nicholson C., Rice M. E., Lindberg J., Zoli M., Agnati L. F. and Fuxe K. (1995) Long distance pathways of diffusion for dextran along fibre bundles in brain. Relevance for volume transmission. *NeuroReport* **6,** 1005–1009.
4. Björklund H. and Dahl D. (1982) Glial disturbances in isolated neocortex: evidence from immunohistochemistry of intraocular grafts. *Devl Neurosci.* **5,** 424–435.
5. Björklund H., Dahl D., Haglid K., Rosengren L. and Olson L. (1983) Astrocytic development in fetal parietal cortex grafted to cerebral and cerebellar cortex of immature rats. *Devl Brain Res.* **9,** 171–180.
6. Bondareff W. and Pysh J. J. (1968) Distribution of extracellular space during postnatal maturation of rat cerebral cortex. *Anat. Rec.* **160,** 773–780.
7. Boschert U., O'Shaughnessy C., Dickinson R., Tessari M., Bendotti C., Catsicas S. and Pich E. M. (1996) Developmental and plasticity-related differential expression of two SNAP-25 isoforms in the rat brain. *J. comp. Neurol.* **367,** 177–193.
8. Bragin A. G., Bohne A. and Vinogradova O. S. (1988) Transplants of the embryonal rat somatosensory neocortex in the barrel field of the adult rat: responses of the grafted neurons to sensory stimulation. *Neuroscience* **25,** 751–758.
9. Buzsáki G., Gage F. H., Kellényi L. and Björklund A. (1987) Behavioral dependence of the electrical activity of intracerebrally transplanted fetal hippocampus. *Brain Res.* **400,** 321–333.
10. Chambers J. M., Cleveland W. S., Kleiner B. and Tukey P. A. (1983) *Graphical Methods for Data Analysis*. Wadsworth and Brooks/Cole, Pacific Grove.
11. Chvátal A., Berger T., Voříšek I., Orkand R. K., Kettenmann H. and Syková E. (1997) Changes in glial K^+ currents with decreased extracellular volume in developing rat white matter. *J. Neurosci. Res.* **49,** 98–106.
12. DeWitt D. A., Richey P. L., Praprotnik P. K., Silver J. and Perry G. (1994) Chondroitin sulfate proteoglycans are a common component of neuronal inclusions and astrocytic reaction in neurodegenerative diseases. *Brain Res.* **656,** 205–209.
13. Dymecki J., Wierzba-Bobrowicz T., Malec I., Medynska E., Poszwinska A. and Stefaniak N. (1990) Development of vessels in the foetal cortical transplant depending on the place of grafting in the rat brain. *Acta neurobiol. exp.* **50,** 397–403.
14. Eddleston M. and Mucke L. (1993) Molecular profile of reactive astrocytes—implications for their role in neurologic disease. *Neuroscience* **54,** 15–36.
15. Friedman B., Hockfield S., Black J. A., Woodruff K. A. and Waxman S. G. (1989) *In situ* demonstration of mature oligodendrocytes and their processes: an immunocytochemical study with a new monoclonal antibody, Rip. *Glia* **2,** 380–390.
16. Fuxe K. and Agnati L. F. (1991) *Volume Transmission in the Brain: Novel Mechanisms for Neural Transmission.* Raven, New York.
17. Galik J., Macias-Gonzalez R., Valoušková V. and Bureš J. (1991) Integration of neocortical embryonic grafts with the neocortex of host rats examined by Leao's spreading cortical depression. *Expl Neurol.* **112,** 321–327.
18. Gates M. A., Laywell E. D., Fillmore H. and Steindler D. A. (1996) Astrocytes and extracellular matrix following intracerebral transplantation of embryonic mesencephalon or lateral ganglionic eminence. *Neuroscience* **74,** 579–597.
19. Girman S. V. and Golovina I. L. (1990) Electrophysiological properties of embryonic neocortex transplants replacing the primary visual cortex of adult rats. *Brain Res.* **523,** 78–86.
20. Harvey A. R. (1994) Expression of low affinity NGF receptors in rat superior colliculus: studies *in vivo*, *in vitro*, and in fetal tectal grafts. *Expl Neurol.* **130,** 237–249.
21. Harvey A. R., Golden G. T. and Lund R. D. (1982) Transplantation of tectal tissue in rats. III. Functional innervation of transplants by host afferents. *Expl Brain Res.* **47,** 437–445.
22. Harvey A. R., Kendall C. L. and Syková E. (1997) The status and organization of astrocytes, oligodendroglia and microglia in grafts of fetal rat cerebral cortex. *Neurosci. Lett.* **227,** 58–62.
23. Harvey A. R. and Lund R. D. (1984) Transplantation of tectal tissue in rats. IV. Maturation of transplants and development of host retinal projection. *Brain Res.* **314,** 27–37.
24. Harvey A. R., Plant G. W. and Kent A. P. (1993) The distribution of astrocytes, oligodendroglia and myelin in normal and transplanted rat superior colliculus: an immunohistochemical study. *J. neural Transplant. Plast.* **4,** 1–14.
25. Jaeger C. B. and Lund R. D. (1981) Transplantation of embryonic occipital cortex to the tectal region of newborn rats: a light microscopic study of organization and connectivity of the transplants. *J. comp. Neurol.* **194,** 571–597.
26. Jaeger C. B. and Lund R. D. (1982) Influence of grafted glia cells and host mossy fibres on anomalously migrated host granule cells surviving in cortical transplants. *Neuroscience* **7,** 3069–3076.
27. Janzer R. C. and Raff M. C. (1987) Astrocytes induce blood–brain barrier properties in endothelial cells. *Nature* **325,** 253–257.
28. Jendelová P. and Syková E. (1991) Role of glia in K^+ and pH homeostasis in the neonatal rat spinal cord. *Glia* **4,** 56–63.
29. Kruger S., Sievers J., Hansen C., Sadler M. and Berry M. (1986) Three morphologically distinct types of interface develop between adult host and fetal brain transplants: implications for scar formation in the adult central nervous system. *J. comp. Neurol.* **249,** 103–116.
30. Krum J. M. and Rosenstein J. M. (1989) The fine structure of vascular–astroglial relations in transplanted fetal neocortex. *Expl Neurol.* **103,** 203–212.
31. Lehmenkühler A., Syková E., Svoboda J., Zilles K. and Nicholson C. (1993) Extracellular space parameters in the rat neocortex and subcortical white matter during postnatal development determined by diffusion analysis. *Neuroscience* **55,** 339–351.
32. Lund R. D. and Harvey A. R. (1981) Transplantation of tectal tissue in rats. I. Organization of transplants and pattern of host afferents within them. *J. comp. Neurol.* **201,** 191–209.
33. Margolis R. U., Aquino D. A., Klinger M. M., Ripellino J. A. and Margolis R. K. (1986) Structure and localization of nervous tissue proteoglycans. *Ann. N.Y. Acad. Sci.* **481,** 46–54.
34. Mazel T., Šimonová Z. and Syková E. (1998) Diffusion heterogeneity and anisotropy in rat hippocampus. *NeuroReport* **9,** 1299–1304.
35. McKeon R. J., Schreiber R. C., Rudge J. S. and Silver J. (1991) Reduction of neurite outgrowth in a model of glial scarring following CNS injury is correlated with the expression of inhibitory molecules on reactive astrocytes. *J. Neurosci.* **11,** 3398–3411.
36. Meiners S., Powell E. M. and Geller H. M. (1995) A distinct subset of tenascin/CS-6-PG-rich astrocytes restricts neuronal growth *in vitro*. *J. Neurosci.* **15,** 8096–8108.
37. Meshul C. K., Seil F. J. and Herndon R. M. (1987) Astrocytes play a role in regulation of synaptic density. *Brain Res.* **402,** 139–145.

38. Muller C. M. (1992) A role for glial cells in activity-dependent central nervous system plasticity? Review and hypothesis. *Int. Rev. Neurobiol.* **34,** 215–281.
39. Neafsey E. J., Sorensen J. C., Tonder N. and Castro A. J. (1989) Fetal cortical transplants into neonatal rats respond to thalamic and peripheral stimulation in the adult. An electrophysiological study of single-unit activity. *Brain Res.* **493,** 33–40.
40. Nicholson C. (1992) Measurement of extracellular space. In *Practical Electrophysiological Methods: A Guide for In Vitro Studies in Vertebrate Neurobiology* (eds Kettenmann H. and Grantyn R.), pp. 367–372. Wiley, New York.
41. Nicholson C. and Phillips J. M. (1981) Ion diffusion modified by tortuosity and volume fraction in the extracellular microenvironment of the rat cerebellum. *J. Physiol., Lond.* **321,** 225–257.
42. Nicholson C. and Syková E. (1998) Extracellular space structure revealed by diffusion analysis. *Trends Neurosci.* **21,** 207–215.
43. Niquet J., Gillian A., Ben-Ari Y. and Represa A. (1996) Reactive glial cells express a vitronectin-like protein in the hippocampus of epileptic rats. *Glia* **16,** 359–367.
44. Palmer M., Björklund H., Olson L. and Hoffer B. (1983) Trophic effects of brain areas on the developing cerebral cortex. II. Electrophysiology of intraocular grafts. *Devl Brain Res.* **6,** 141–148.
45. Pfrieger F. F. and Barres B. A. (1996) New views on synapse–glia interactions. *Curr. Opin. Neurobiol.* **6,** 615–621.
46. Pike C. J., Cummings B. J. and Cotman C. W. (1995) Early association of reactive astrocytes with senile plaques in Alzheimer's disease. *Expl Neurol.* **132,** 172–179.
47. Prokopová Š., Nicholson C. and Syková E. (1996) The effect of 40-kDa or 70-kDa dextran and hyaluronic acid solution on extracelluar space tortuosity in isolated rat spinal cord. *Physiol. Res.* **45,** P28.
48. Prokopová Š., Vargová L. and Syková E. (1997) Heterogeneous and anisotropic diffusion in the developing rat spinal cord. *NeuroReport* **8,** 3527–3532.
49. Pysh J. J. (1969) The development of the extracellular space in neonatal rat inferior colliculus an electron microscopic study. *Am. J. Anat.* **124,** 411–430.
50. Ransom B. R., Carlini W. G. and Connors B. W. (1985) Brain extracellular space: developmental studies in rat optical nerve. *Ann. N.Y. Acad. Sci.* **481,** 87–105.
51. Rice M. E., Okada Y. C. and Nicholson C. (1993) Anisotropic and heterogeneous diffusion in the turtle cerebellum: implications for volume transmission. *J. Neurophysiol.* **70,** 2035–2044.
52. Roitbak T., Šimonová Z. and Syková E. (1998) Increase in extracellular space volume and tortuosity during astrogliosis in rat cortex. European Meeting on Glial Cell Function in Health and Disease, Athens, 146.
53. Rosenstein J. M. (1995) Diminished expression of microtubule-associated protein (MAP-2) and beta-tubulin as a putative marker for ischemic injury in neocortical transplants. *Cell Transplant.* **4,** 83–91.
54. Rosenstein J. M. (1995) Why do neural transplants survive? An examination of some metabolic and pathophysiological considerations in neural transplantation. *Expl Neurol.* **133,** 1–6.
55. Sabel M., Bele S., Gass P., Sommer C. and Kiessling M. (1995) Developmental expression of GAP-43 and SNAP-25 in heterotopic rat cortical grafts. *Neurosci. Lett.* **189,** 151–154.
56. Segal M. and Azmitia E. C. (1986) Fetal raphe neurons grafted into the hippocampus develop normal adult physiological properties. *Brain Res.* **363,** 162–166.
57. Šimonová Z., Svoboda J., Orkand R., Bernard C. C. A., Lassmann H. and Syková E. (1996) Changes of extracellular space volume and tortuosity in the spinal cord of Lewis rats with experimental autoimmune encephalomyelitis. *Physiol. Res.* **45,** 11–22.
58. Siviy S. M., Walsh J. P., Radisavljevic Z., Cohen R. W., Buchwald N. A. and Levine M. S. (1993) Evidence for enhanced synaptic excitation in transplanted neostriatal neurons. *Expl Neurol.* **123,** 222–234.
59. Smith G. M., Jacobberger J. W. and Miller R. H. (1993) Modulation of adhesion molecule expression on rat cortical astrocytes during maturation. *J. Neurochem.* **60,** 1453–1466.
60. Soares H. and McIntosh T. K. (1991) Fetal cortical transplants in adult rats subjected to experimental brain injury. *J. neural Transplant. Plast.* **2,** 207–220.
61. Swenson R. S., Shaw P., Alones V., Kozlowski G., Zimmer J. and Castro A. J. (1989) Neocortical transplants grafted into the newborn rat brain demonstrate a blood–brain barrier to macromolecules. *Neurosci. Lett.* **100,** 35–39.
62. Syková E. (1997) The extracellular space in the CNS: its regulation, volume and geometry in normal and pathological neuronal function. *Neuroscientist* **3,** 28–41.
63. Syková E., Jendelová P., Šimonová Z. and Chvátal A. (1992) K^+ and pH homeostasis in the developing rat spinal cord is impaired by early postnatal X-irradiation. *Brain Res.* **594,** 19–30.
64. Syková E., Svoboda J., Polák J. and Chvátal A. (1994) Extracellular volume fraction and diffusion characteristics during progressive ischemia and terminal anoxia in the spinal cord of the rat. *J. cerebr. Blood Flow Metab.* **14,** 301–311.
65. Syková E., Svoboda J., Šimonová Z., Lehmenkühler A. and Lassmann H. (1996) X-irradiation-induced changes in the diffusion parameters of the developing rat brain. *Neuroscience* **70,** 597–612.
66. Tao L. and Nicholson C. (1996) Diffusion of albumins in rat cortical slices and relevance to volume transmission. *Neuroscience* **75,** 839–847.
67. Vořišek I. and Syková E. (1997) Evolution of anisotropic diffusion in the developing rat corpus callosum. *J. Neurophysiol.* **78,** 912–919.
68. Vořišek I. and Syková E. (1997) Ischemia-induced changes in the extracellular space diffusion parameters, K^+ and pH in the developing rat cortex and corpus callosum. *J. cerebr. Blood Flow Metab.* **17,** 191–203.
69. Zimmer J. and Sunde N. (1984) Neuropeptides and astroglia in intracerebral hippocampal transplants. An immunohistochemical study in the rat. *J. comp. Neurol.* **227,** 331–347.

(*Accepted* 5 *October* 1998)